

# Intrinsic stability of quantum cascade lasers against optical feedback

F. P. Mezzapesa,<sup>1,2,\*</sup> L. L. Colombo,<sup>1,3</sup> M. Brambilla,<sup>1,2</sup> M. Dabbicco,<sup>1,2</sup> S. Borri,<sup>1</sup>  
M. S. Vitiello,<sup>4</sup> H. E. Beere,<sup>5</sup> D. A. Ritchie,<sup>5</sup> and G. Scamarcio<sup>1,2</sup>

<sup>1</sup>CNR-IFN UOS Bari, via Amendola 173, I-70126 Bari, Italy

<sup>2</sup>Dipartimento Interateneo di Fisica, Università degli Studi e Politecnico di Bari, via Amendola 173, I-70126 Bari, Italy

<sup>3</sup>Dipartimento di Scienza ed Alta tecnologia, Università dell'Insubria, via Valleggio 11, 22100 Como, Italy

<sup>4</sup>NEST, CNR - Istituto Nanoscienze and Scuola Normale Superiore, Piazza San Silvestro 12, 56127 Pisa, Italy

<sup>5</sup>Cavendish Laboratory, University of Cambridge, J. J. Thomson Avenue, Cambridge CB3 0HE, UK

\*francesco.mezzapesa@uniba.it

**Abstract:** We study the time dependence of the optical power emitted by terahertz and mid-IR quantum cascade lasers in presence of optical reinjection and demonstrate unprecedented continuous wave (CW) emission stability for strong feedback. We show that the absence of coherence collapse or other CW instabilities typical of diode lasers is inherently associated with the high value of the photon to carrier lifetime ratio and the negligible linewidth enhancement factor of quantum cascade lasers.

©2013 Optical Society of America

**OCIS codes:** (140.5965) Semiconductor lasers, quantum cascade; (140.3430) Laser theory; (140.3425) Laser stabilization; (030.1640) Coherence; (140.3070) Infrared and far-infrared lasers.

---

## References and links

1. J. Faist, F. Capasso, D. L. Sivco, C. Sirtori, A. L. Hutchinson, and A. Y. Cho, "Quantum cascade laser," *Science* **264**(5158), 553–556 (1994).
2. R. Köhler, A. Tredicucci, F. Beltram, H. E. Beere, E. H. Linfield, A. G. Davies, D. A. Ritchie, R. C. Iotti, and F. Rossi, "Terahertz semiconductor-heterostructure laser," *Nature* **417**(6885), 156–159 (2002).
3. B. S. Williams, "Terahertz quantum-cascade lasers," *Nat. Photonics* **1**(9), 517–525 (2007).
4. M. S. Vitiello and A. Tredicucci, "Tunable emission in a THz quantum cascade lasers," *IEEE Trans. Terahertz Sci. Technol.* **1**(1), 76–84 (2011).
5. M. Tonouchi, "Cutting edge terahertz technology," *Nat. Photonics* **1**(2), 97–105 (2007).
6. R. F. Curl, F. Capasso, C. Gmachl, A. A. Kosterev, B. Mc Manus, R. Lewicki, M. Pusharsky, G. Wysocki, and F. K. Tittel, "Quantum cascade lasers in chemical physics," *Chem. Phys. Lett.* **487**(1-3), 1–18 (2010).
7. Y. I. Khanin, in *Principles of Laser Dynamics* (Elsevier, 1995).
8. R. Paiella, R. Martini, F. Capasso, C. Gmachl, H. Y. Hwang, D. L. Sivco, J. N. Baillargeon, A. Y. Cho, E. A. Whittaker, and H. C. Liu, "High-frequency modulation without the relaxation oscillation resonance in quantum cascade lasers," *Appl. Phys. Lett.* **79**(16), 2526–2528 (2001).
9. S. Barbieri, M. Ravano, P. Gellie, G. Santarelli, C. Manquest, C. Sirtori, S. P. Khanna, H. Linfield, and A. G. Davies, "Coherent sampling of active mode-locked terahertz quantum cascade lasers and frequency synthesis," *Nat. Photonics* **5**(5), 306–313 (2011).
10. C. Y. Wang, L. Kuznetsova, V. M. Gkortsas, L. Diehl, F. X. Kärtner, M. A. Belkin, A. Belyanin, X. Li, D. Ham, H. Schneider, P. Grant, C. Y. Song, S. Haffouz, Z. R. Wasilewski, H. C. Liu, and F. Capasso, "Mode-locked pulses from mid-infrared quantum cascade lasers," *Opt. Express* **17**(15), 12929–12943 (2009).
11. N. Yu, L. Diehl, E. Cubukcu, D. Bour, S. Corzine, G. Höfler, A. K. Wojcik, K. B. Crozier, A. Belyanin, and F. Capasso, "Coherent Coupling of Multiple Transverse Modes in Quantum Cascade Lasers," *Phys. Rev. Lett.* **102**(1), 013901 (2009).
12. A. Gordon, C. Y. Wang, L. Diehl, F. X. Kärtner, A. Belyanin, D. Bour, S. Corzine, G. Höfler, H. C. Liu, H. Schneider, T. Maier, M. Troccoli, J. Faist, and F. Capasso, "Multimode regimes in quantum cascade lasers: From coherent instabilities to spatial hole burning," *Phys. Rev. A* **77**(5), 053804 (2008).
13. R. Paiella, F. Capasso, C. Gmachl, D. L. Sivco, J. N. Baillargeon, A. L. Hutchinson, A. Y. Cho, and H. C. Liu, "Self-Mode-Locking of Quantum Cascade Lasers with Giant Ultrafast Optical Nonlinearities," *Science* **290**(5497), 1739–1742 (2000).
14. L. Consolino, A. Taschin, P. Bartolini, S. Bartalini, P. Cancio, A. Tredicucci, H. E. Beere, D. A. Ritchie, R. Torre, M. S. Vitiello, and P. De Natale, "Phase-locking to a free-space terahertz comb for metrological-grade terahertz lasers," *Nat Commun* **3**, 1040 (2012).

15. J. Kroll, J. Darmo, K. Unterrainer, S. Dhillon, C. Sirtori, X. Marcadet, and M. Calligaro, "Longitudinal spatial hole burning in terahertz quantum cascade lasers," *Appl. Phys. Lett.* **91**(16), 161108 (2007).
16. D. M. Kane and K. A. Shore, in *Unlocking Dynamical Diversity – Optical Feedback Effects on Semiconductor Diode Lasers* (J. Wiley and Sons, 2005).
17. P. Dean, Y. L. Lim, A. Valavanis, R. Kliese, M. Nikolić, S. P. Khanna, M. Lachab, D. Indjin, Z. Ikonić, P. Harrison, A. D. Rakić, E. H. Linfield, and A. G. Davies, "Terahertz imaging through self-mixing in a quantum cascade laser," *Opt. Lett.* **36**(13), 2587–2589 (2011).
18. Y. L. Lim, P. Dean, M. Nikolić, R. Kliese, S. P. Khanna, M. Lachab, A. Valavanis, D. Indjin, Z. Ikonić, P. Harrison, E. Linfield, A. G. Davies, S. J. Wilson, and A. D. Rakić, "Demonstration of a self-mixing displacement sensor based on terahertz quantum cascade lasers," *Appl. Phys. Lett.* **99**(8), 081108 (2011).
19. M. C. Phillips and M. S. Taubman, "Intracavity sensing via compliance voltage in an external cavity quantum cascade laser," *Opt. Lett.* **37**(13), 2664–2666 (2012).
20. F. P. Mezzapesa, V. Spagnolo, A. Antonio, and G. Scamarcio, "Detection of ultrafast laser ablation using quantum cascade laser-based sensing," *Appl. Phys. Lett.* **101**(17), 171107 (2012).
21. J. Helms and K. Petermann, "A simple analytic expression for the stable operation range of laser diodes with optical feedback," *IEEE J. Quantum Electron.* **26**(5), 833–836 (1990).
22. R. P. Green, J. H. Xu, L. Mahler, A. Tredicucci, F. Beltram, G. Giuliani, H. E. Beere, and D. A. Ritchie, "Linewidth enhancement factor of terahertz quantum cascade lasers," *Appl. Phys. Lett.* **92**(7), 071106 (2008).
23. R. Lang and K. Kobayashi, "External optical feedback effects on semiconductor injection laser properties," *IEEE J. Quantum Electron.* **16**(3), 347–355 (1980).
24. R. W. Tkach and A. R. Chraplyvy, "Regimes of feedback effects in 1.5 $\mu$ m distributed feedback lasers," *J. Lightwave Technol.* **4**(11), 1655–1661 (1986).
25. B. Tromborg, J. H. Osmundsen, and H. Olesen, "Stability Analysis for a Semiconductor Laser in an External Cavity," *IEEE J. Quantum Electron.* **20**(9), 1023–1032 (1984).
26. M. Yamanishi, T. Edamura, K. Fujita, N. Akikusa, and H. Kan, "Theory of the intrinsic linewidth of quantum cascade lasers: hidden reason for the narrow linewidth and line broadening by thermal photons," *IEEE J. Quantum Electron.* **44**(1), 12–29 (2008).
27. M. S. Vitiello, L. Consolino, S. Bartalini, A. Taschin, A. Tredicucci, M. Inguscio, and P. De Natale, "Quantum limited frequency fluctuations in a terahertz laser," *Nat. Photonics* **6**(8), 525–528 (2012).
28. D. Weidmann, K. Smith, and B. Ellison, "Experimental investigation of high-frequency noise and optical feedback effects using a 9.7 microm continuous-wave distributed-feedback quantum-cascade laser," *Appl. Opt.* **46**(6), 947–953 (2007).

## 1. Introduction

Terahertz and mid-infrared Quantum Cascade Lasers (QCLs) are semiconductor sources capable of emitting infrared radiation in the frequency ranges 1-5 THz and 15-100 THz, respectively [1, 2]. Since their first demonstration, researches flourished, focusing on the design optimization and steady-state features such as lasing threshold, tunability, operating temperature, waveguide coupling, and output power [3, 4]. Hence, QCLs are suited for many relevant applications including, but not limited to, imaging, communications technology, sensing, molecular gas spectroscopy, biological and medical sciences, astrophysics and space-science [5, 6]. The lasing emission relies on intersubband transitions in the conduction band of atomically sharp heterostructures, in which the carrier lifetime is dominated by non-radiative phonon scattering phenomena and thus it falls into the range of picoseconds, about  $10^2$  -  $10^3$  times shorter than typical values for interband semiconductor lasers. This ultrafast mechanism makes the QCL the only solid-state laser belonging to the group of class-A lasers, where the carrier density and the macroscopic polarization are enslaved by the electromagnetic field [7]. Consequently, QCLs show an overdamped transient dynamics towards the steady-state, which allows for instance intrinsic modulation bandwidths up to several tens of GHz, with appealing applications in the field of free-space optical communication [8]. The search for ultrafast high-intensity pulse trains has motivated several works focusing on QCLs dynamics [9–14], and aiming at applications such as frequency comb generation, time-resolved measurement, and nonlinear wavelength conversion. A focus lies on multimode regimes due to instabilities that are typical of multiple longitudinal mode QCLs, and mainly to coherent mechanisms such as the Risken-Nummedal-Graham-Haken instability and the spatial hole burning [12, 15]. Such mechanisms are readily observable in intersubband lasers because of their picosecond carrier lifetime, which favors the onset of

complex multimode dynamics, although preventing at the same time conventional mode locking, i.e. with one pulse per round-trip.

The absence of an intrinsic system resonance at the relaxation frequency is also expected to affect the dynamical behavior of QCLs under optical feedback (OF), since the amplification of the relaxation frequency under increasing feedback power is one of the main causes of laser instability [16]. QCLs with optical feedback have recently witnessed an increasing interest, aimed to applications such as sensing, imaging and spectroscopy, in which the laser source is used to simultaneously generate and detect the radiation in self-mixing (SM) configuration [17–20]. SM occurs when the laser radiation is reflected or diffused from an external target and fed back into the laser cavity. In the general class of semiconductor lasers, external optical feedback is known to influence steady-state features, as e.g. lasing threshold, emitted power, spectral purity and relative intensity noise. It can also lead to peculiar complex dynamics, including route to chaos, laser pulsing, coherence collapse, etc., which have been largely investigated on both the theoretical and experimental side in bipolar semiconductor lasers [16, 21 and ref. therein]. Yet, the understanding of QCL dynamics in presence of OF is still in its infancy. Furthermore, there is theoretical evidence that the sensitivity to optical feedback of a semiconductor laser also depends on the linewidth enhancement factor ( $\alpha$ ), which couples the material gain with the refractive index. In particular,  $\alpha$  close to zero are predicted to prevent coherent collapse [21] and this is precisely the case of THz QCLs, whose symmetric differential gain induces a value of  $\alpha < 1$ , as recently measured [22]. Accordingly, the combined effect of small linewidth enhancement factors and high photon-to-carrier lifetime ratios make unipolar semiconductor lasers, such as QCLs, ideal candidates to show enhanced stability in OF configurations under strong feedback. Self-consistent theories and more systematic experimental investigations are therefore required to fully understand and exploit OF-related phenomena in technological applications based on QCLs.

In this work, the intrinsic stability of continuous wave emission in optically re-injected THz QCLs is theoretically predicted and experimentally supported. We model the laser with optical feedback by the semiconductor Lang-Kobayashi (LK) equations [23] and the numerical results unambiguously show the disappearance of coherence collapse in THz QCLs due to undamped relaxation oscillations. Similar results are obtained with a strongly re-injected mid-infrared QCL. We ascribe the intrinsic stability to the high value of their photon to carrier lifetime ratio and to the negligible linewidth enhancement factor. Significantly, we report the experimental evidence of stable CW emission both in THz and mid-IR QCLs for feedback levels up to two orders of magnitude higher than the feedback threshold causing coherence collapse in bipolar diodes in an equivalent SM configuration.

## 2. Laser dynamics and basic steady state properties

The standard form of the LK model as written in Eq. (7.4) of [16] can be rescaled by introducing the field  $E = \tilde{E} \sqrt{G_n \tau_e}$ , the carrier density  $N = (\tilde{N} - \tilde{N}_0) G_n \tau_p$  and the pump parameter  $I_p = G_n \tau_p \tilde{N}_0 (G_{gen} \tau_e / \tilde{N}_0 - 1)$ , and cast as:

$$\frac{dE(t)}{dt} = \frac{1}{2} (1 + i\alpha) (N(t) - 1) E(t) + \frac{k \tau_p}{\tau_c} E(t - \tau) e^{i a_0 \tau} \quad (1)$$

$$\frac{dN(t)}{dt} = \mathcal{H}[I_p - N(t)(1 + |E(t)|^2)] \quad (2)$$

where  $\tilde{E}(t)$  and  $\tilde{N}(t)$  are the slowly varying envelopes of the electric field and carriers density, respectively;  $\tilde{N}_0$  is the carrier density at transparency;  $G_n$  is the modal gain

coefficient;  $G_{gen}$  is the electrical pumping term;  $\tau_e$  is the non-radiative carriers lifetime;  $\tau_p$  is the photon lifetime;  $\tau_c$  is the laser cavity round trip time, and  $\tau = 2L/c$  is the round trip time in the external cavity of length  $L$ .  $\omega_0$  is the solitary laser frequency (where the laser cavity resonance is the reference frequency);  $k$  is the feedback strength parameter and  $\gamma$  is the photon to carrier lifetime ratio. The time  $t$  in Eqs. (1) and (2) is expressed in units of  $\tau_p$ .

Looking for CW solutions of Eqs. (1) and (2) in the form  $E(t) = E_s \exp[i(\omega_F - \omega_0)t]$  and  $N(t) = N_s$ , we get:

$$N_s = 1 - 2k \frac{\tau_p}{\tau_c} \cos(\omega_F \tau) |E_s|^2 = \frac{I_p}{N_s} - 1; \omega_F = \omega_0 - (k \frac{\tau_p}{\tau_c}) [\alpha \cos(\omega_F \tau) + \sin(\omega_F \tau)] \quad (3)$$

From Eq. (3) it follows that the steady state characteristic of a re-injected semiconductor laser may be strongly affected by the optical feedback. Relevant for the experimental measurements of the optical feedback level is the following relation between the pump intensity at threshold in presence of feedback,  $(I_p)_{th}$ , and the pump intensity at threshold for the solitary laser,  $(I_{ps})_{th} = 1$ :

$$(I_p - I_{ps})_{th} = -(2k \frac{\tau_p}{\tau_c}) \cos(\omega_F \tau) \quad (4)$$

where the feedback strength parameter depends on the effective fraction of the back-reflected field re-entering the laser, the laser exit facet and the external mirror reflectivity.

### 3. Experimental results

We consider the SM configuration sketched in Fig. 1 where a semiconductor laser is subject to optical reinjection provided by an external target.

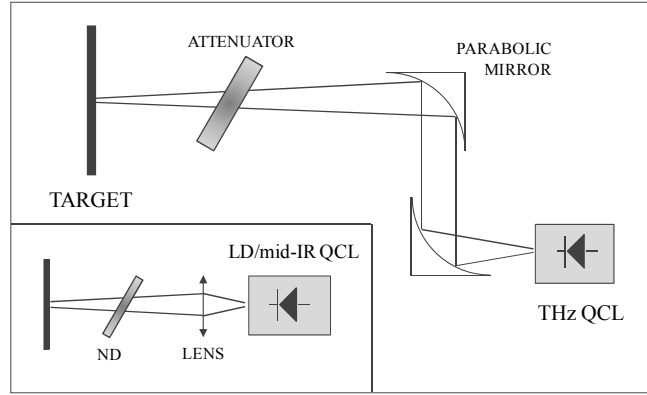


Fig. 1. Schematic layout of the experimental configuration. The THz QCL radiation is focused on the external target (a metallic mirror) and re-injected into the laser cavity. The inset shows the equivalent configuration with a mid-IR QCL or a conventional laser diode (LD). ND: neutral density filter. TPX foils are used as attenuator with QCLs.

A resonant phonon single longitudinal mode THz QCL emitting at the wavelength of  $76.3 \mu\text{m}$  (3.93 THz) with a surface plasmon waveguide, was grown by molecular beam epitaxy employing a GaAs/ $\text{Al}_{0.15}\text{Ga}_{0.85}\text{As}$  heterostructure on a nominally undoped GaAs substrate. The active region was engineered with two upper laser levels closely separated by about 1 meV energy. Because of the two upper states, the dipole matrix element of each transition is smaller ( $\sim 5 \text{ nm}$ ) than what typical for standard THz QCLs emitting at the same frequency. A 500 nm thick layer heavily doped ( $3.0 \times 10^{18} \text{ cm}^{-3}$ , Si) defines the lower contact of laser. The

active region is repeated 120 times and the growth ends with a heavily doped ( $5.0 \times 10^{18} \text{ cm}^{-3}$ , Si) GaAs (200 nm) contact layer. Lasing at 3.8 THz with a threshold current density of  $82 \text{ A/cm}^2$  at 5 K was demonstrated. The maximum output power is achieved near  $400 \text{ A/cm}^2$ , still 2.5-3 times above threshold. Lasing is observed in pulsed mode up to 70 K with a peak power level in excess of 30 mW at 10 K.

The investigated THz QCL was mounted on the cold finger of a continuous-flow cryostat fitted with a polymethylpentene (TPX) window and kept at an heat sink temperature of 15 K. In our experiment, the THz QCL was driven at a constant current  $I = 710 \text{ mA}$  for CW mode operation. The THz QCL beam was collimated using a 2 inch  $f/2 = 25.4 \text{ mm}$   $90^\circ$  off-axis paraboloidal reflector and focused by a second reflector of 2 inch  $f/2 = 76.2 \text{ mm}$  at normal incidence onto the remote target (reflectivity of 75% at  $\sim 4 \text{ THz}$ ). The laser beam was then coupled back into the laser cavity along an optical path of 365 mm (i.e., distance between the source and the target) and the feedback strength was changed by means of a variable attenuator. Coherent self-mixing of the reflected beam with the optical field inside the laser cavity, as depending on their relative phase difference, causes a voltage change on the laser terminals at the current controller. The effect of feedback - SM signal - was measured as voltage modulation across the device. The voltage offset measured across the device was subtracted by ac-coupling to a low noise amplifier with a gain of 40 dB. In this voltage sensing configuration, the THz QCL worked as source and detector of radiation, therefore no output coupling was required. Note that, to maximize both the QCL sensitivity to optical feedback and the back-coupling in the laser cavity, we operate with a QCL driving current 6% larger than its threshold value [17] and in a self-imaging configuration, respectively.

The inset in Fig. 1 shows a schematic sketch of the experimental apparatus implemented to investigate the dynamical behavior of a mid-IR QCL and a conventional laser diode (LD) under optical re-injection. A tunable single mode mid-IR QCL working at a wavelength of  $6.24 \mu\text{m}$  (Alpes Lasers, mod. RT-CW-DFB-QCL) was driven at  $I = 515 \text{ mA}$  (6% above threshold) for CW operation and temperature stabilized at 283 K. The probe beam emitted from the QCL was collimated by an AR-coated aspheric lens (chalcogenide glass) of nominal focal length  $f = 4 \text{ mm}$  with high numerical aperture ( $\text{NA} = 0.56$ ).

Similarly, a single longitudinal mode laser diode (Hitachi HL8325G) emitting at a wavelength of 832 nm was driven by a high compliance current controller (not shown in Fig. 1) at a constant current  $I = 42.5 \text{ mA}$  for CW operation (6% above threshold). The radiation emitted from the LD was collimated by an AR-coated aspheric lens of  $f = 11 \text{ mm}$  and  $\text{NA} = 0.25$ . A set of neutral density filters allowed to adjust the effective optical feedback reflected off the target surface and focused on the laser front facet. This feedback radiation eventually modulates the optical power, as detected by the voltage change on the QCL terminals or by the monitor photodiode packaged into the laser diode, respectively. In the latter case, the laser response to the feedback effect was measured as photocurrent modulation, and ac-coupled to a transimpedance amplifier having gain  $G = 10^4 \text{ V/A}$ .

The spectral power density of the SM signals of a THz QCL, a mid-IR QCL and a diode laser subject to different values of the optical feedback strength has been retrieved by analyzing the associated SM signals, as shown in Fig. 2. We introduce a novel technique to experimentally assess the feedback strength parameter. Specifically, we derive  $k$  from Eq. (4) by accurately measuring the current threshold variation induced by the back-reflected light.

Figure 2(a) shows a representative power spectrum of the SM signal, as measured by carefully aligning the target in Fig. 1 to maximize the radiation feedback strength in the THz QCL cavity, and removing the attenuation. At any feedback level, no transition to typical CW instabilities such as mode-hopping, intensity pulsation or coherence collapse [24], can be observed. Moreover, the stable CW emission of the THz QCL was evidenced for a feedback strength as high as  $k = 7.5 \times 10^{-2}$ , which is the maximum feedback level obtainable for a quantum cascade laser in our SM configuration. Also, we observed similar stable behavior in the case of the mid-infrared QCL for a maximum  $k = 6.8 \times 10^{-2}$ , as shown in Fig. 2(b).

This behavior is radically different from that of conventional bipolar semiconductor lasers. In fact, Figs. 2(c) and 2(d) show the power spectra of the self-mixing signal as measured by varying the external feedback re-injected into the LD cavity. A clear signature of the coherence collapse regime in the LD laser is given in Fig. 2(c) for a feedback strength parameter  $k = 1.1 \times 10^{-3}$ , as depicted by a two order of magnitude rise in the continuous FFT of the SM spectrum. Remarkably, this value of  $k$  is almost one hundred times smaller than the maximum feedback strength achievable in our QCLs and still yielding to a stable CW emission. Lowering the strength to  $k = 0.8 \times 10^{-3}$  restores the stable regime (see Fig. 2(d)). Similar results are expected in any class of diode lasers [16].

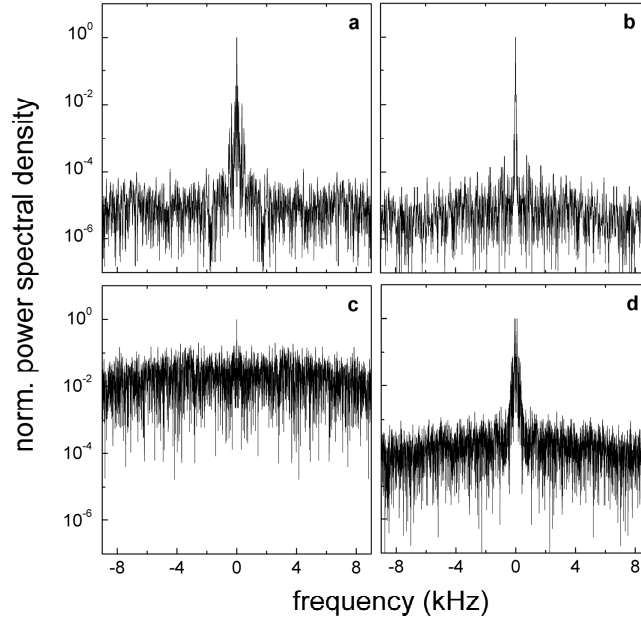


Fig. 2. Normalized FFT (Blackman window weighting approximation) of representative oscilloscope traces showing the time dependence of the SM signals detected by: (a) voltage modulation at the THz QCL terminals; (b) voltage modulation at the mid-IR QCL terminals; (c)-(d) LD integrated photodiode. Figure 2(a): stable CW emission of THz QCL subject to the maximum feedback strength, i.e. for  $k = 7.5 \times 10^{-2}$ . Figure 2(b): stable CW operation of the mid-IR QCL at the maximum feedback strength, i.e. for  $k = 6.8 \times 10^{-2}$ . Figures 2(c) and 2(d): coherence collapse ( $k = 1.1 \times 10^{-3}$ ) and stable CW emission ( $k = 0.8 \times 10^{-3}$ ) in a diode laser, respectively.

### 3. Stability analysis and discussion

In order to explain the intrinsic stability of QCLs under OF and clarify the role played by the linewidth enhancement factor and the photon to carrier lifetime ratio, we performed a semi-analytical linear stability analysis (LSA) of the steady state to determine the limits of stable operation and simulate the laser dynamics by numerically integrating the delayed rate-equations (i.e., Eqs. (1) and (2)), as shown in Fig. 3.

Assuming perturbations  $\delta E(t) = \delta E_0(t) \exp[\lambda t + i(\omega_F - \omega_0)t]$  and  $\delta N(t) = \delta N_0(t) \exp(\lambda t)$  to the CW values in Eq. (3), we obtain by linearization a transcendental equation for the complex exponent  $\lambda$ :

$$\lambda^3 + a_2(\lambda)\lambda^2 + a_1(\lambda)\lambda + a_0(\lambda) = 0 \quad (5)$$

where the coefficients are:

$$a_2 = \gamma \frac{I_p}{N_s} + 2 \frac{k \tau_p}{\tau_c} (1 - e^{-\lambda \tau}) \cos(\omega_F \tau) \quad (6.a)$$

$$a_1 = \gamma \left[ 2 \frac{I_p k \tau_p}{N_s \tau_c} (1 - e^{-\lambda \tau}) \cos(\omega_F \tau) + E_s^2 N_s \right] + \left[ \frac{k \tau_p}{\tau_c} (1 - e^{-\lambda \tau}) \right]^2 \quad (6.b)$$

$$a_0 = \gamma \left\{ \left[ \frac{E_s^2 N_s k \tau_p}{\tau_c} (1 - e^{-\lambda \tau}) [\cos(\omega_F \tau) - \alpha \sin(\omega_F \tau)] + \frac{I_p}{N_s} \left[ \frac{k \tau_p}{\tau_c} (1 - e^{-\lambda \tau}) \right]^2 \right\} \right. \quad (6.c)$$

All the solutions of Eq. (5) must have a negative real part for a CW emission to be stable. It can be numerically studied to find the minimum value of  $k$  for an instability to set on, i.e. yielding  $\max \text{Re}(\lambda) = 0$ , hereinafter called the critical feedback strength,  $k_c$ . We note that in the limit of  $\gamma \gg 1$ , valid for quantum cascade lasers, Eq. (5) can be reduced to a simpler form:

$$\lambda^2 + b_1(\lambda)\lambda + b_0(\lambda) = 0 \quad (7)$$

where the coefficients are:

$$b_1 = 2 \frac{k \tau_p}{\tau_c} (1 - e^{-\lambda \tau}) \cos(\omega_F \tau) + \frac{E_s^2 N_s^2}{I_p} \quad (8.a)$$

$$b_0 = \frac{E_s^2 N_s^2 k \tau_p}{I_p \tau_c} (1 - e^{-\lambda \tau}) [\cos(\omega_F \tau) - \alpha \sin(\omega_F \tau)] + \left[ \frac{k \tau_p}{\tau_c} (1 - e^{-\lambda \tau}) \right]^2 \quad (8.b)$$

Figure 3(a) shows the radical increase of the critical feedback strength with the photon to carrier lifetime ratio, and the fundamental change of the instability character when  $\gamma > 1$ . Note that the simulation parameters are typical of a laser diode. The reduction of this set, and of  $\alpha$  in particular, to the case of QCLs will be treated in the following.

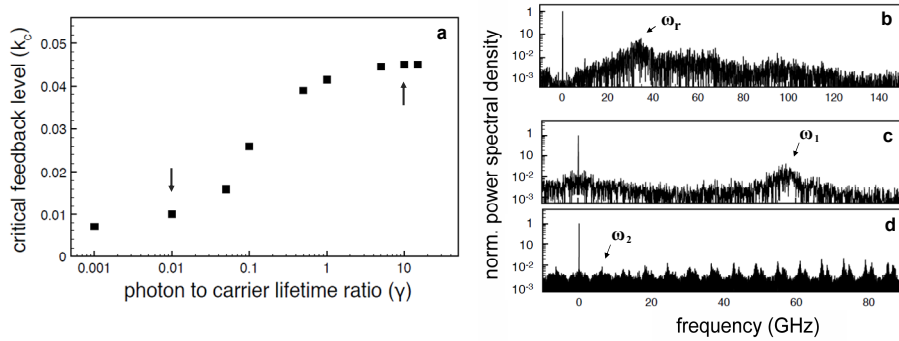


Fig. 3. Results of LSA from the numerical solution of Eq. (5), coinciding with the Eq. (7) for  $\gamma \gg 1$ . In Fig. 3(a) we plot the critical  $k_c$  vs  $\gamma$  obtained for typical laser diode parameters (i.e.  $\alpha = 5$ ;  $\tau_c = 3.8$  ps;  $\tau_p = 3.3$  ps;  $\lambda_{LD} = 832$  nm;  $L = 14$  mm). For  $\gamma < 1$ , the critical feedback level monotonically increases; these instabilities are associated to undamped relaxation oscillations, as representatively shown in Fig. 3(b) for  $\gamma = 0.01$  and  $I_p = 2.5$  (note that the pump threshold is  $(I_p)_{th} = 1$ ): the undamped relaxation frequency is  $\omega_r \approx 35$  GHz. For  $\gamma > 1$ , the critical feedback level saturates at  $k_c = 0.045$ , beyond which the unstable regime is due to external cavity mode competition, as representatively shown in Figs. 3(c) and 3(d) for  $\gamma = 10$  and  $I_p = 1.5$ : the beating frequencies are at multiples of  $\omega_1 \approx 60$  GHz (panel c) and  $\omega_2 \approx 6$  GHz (panel d) for an external cavity length of 14 and 140 mm, respectively. In the latter case, i.e. for  $\omega_2 \approx 6$  GHz, ten external modes are present in the frequency range covering one free spectral range of the former case, as expected.

For  $\gamma < 1$ , the critical feedback level increases with  $\gamma$ , which is realistic for a bipolar laser since the instabilities are caused by the undamped relaxation oscillations, whose frequency, associated to the imaginary part of the unstable eigenvalues  $\lambda$ , depends on  $\gamma$  [21, 25]. To confirm this picture, in a CW unstable regime we verified the onset of the continuous component in the Fourier spectrum of the field intensity  $|E(t)|^2$  (see Fig. 3(b)) related to the transition to the coherence collapse. The simulation also shows the existence of peaks at the relaxation oscillation frequency (see  $\omega_r$  in the panel), which could not be revealed in the experiment due to bandwidth limitation.

For  $\gamma > 1$  (a carrier lifetime approximately ten times smaller than the photon lifetime is typical of QCLs), the relaxation oscillations are suppressed, as mentioned above. In Fig. 3(a), though, we see  $k_C$  approaching an almost constant value; obviously the instability emerging beyond  $k_C$  must have a different origin. In fact, our numerical simulations show peaks in the power spectrum (see Figs. 3(c) and 3(d)) separated by multiples of the external cavity free spectral range. This proves the competition among external cavity resonances. We also verified that by varying the cavity length from 14 to 140 mm (i.e.  $\omega_1 \approx 60$  GHz and  $\omega_2 \approx 6$  GHz, respectively), the same dynamical behavior is found (Fig. 3(d)).

However, in the THz QCL experiment no instabilities were observed at any feedback level, i.e. for  $k$ -value at least two orders of magnitude higher than the laser diode case. Therefore, an additional mechanism must be invoked to account for the intrinsic stability. We infer that a small value of the  $\alpha$ -factor in THz quantum cascade lasers (typically less than one [26], as recently measured [22, 27]) is responsible of this unique behavior.

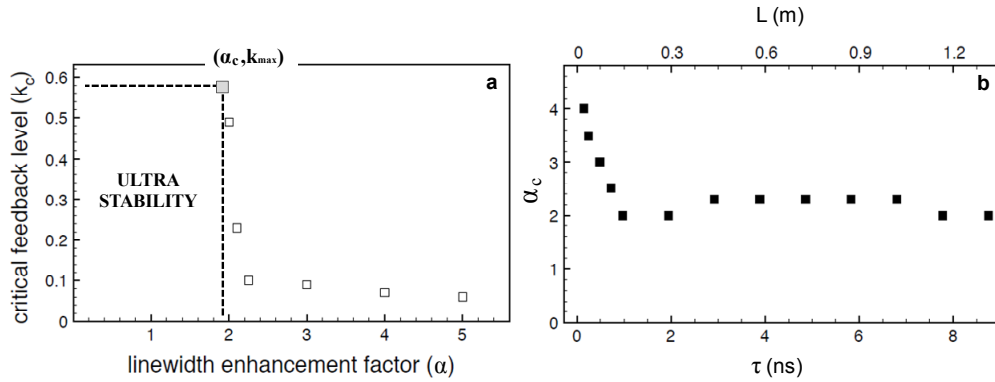


Fig. 4. THz QCL ultra stability under optical re-injection: results of numerical simulations. Figure 4(a): minimum feedback strength for the onset of CW instability vs  $\alpha$  for realistic parameters of a THz QCL. The critical feedback level increases with decreasing  $\alpha$  up to  $k_{\max} = \tau_c/2\tau_p = 0.58$ , corresponding to a critical linewidth enhancement factor ( $\alpha_c$ ). Ultra stable dynamics under optical re-injection are predicted for  $\alpha < \alpha_c$ . Figure 4(b): plot of  $\alpha_c$  vs the external cavity round trip time ( $\tau = 2L/c$ ). The other parameters are:  $\gamma = 10$ ;  $\tau_c = 37.4$  ps;  $\tau_p = 32.4$  ps;  $\lambda_{\text{THz-QCL}} = 76 \mu\text{m}$ ;  $L = 140$  mm.

To this purpose, we determined the boundaries of the CW stable domain as a function of the linewidth enhancement factor, as representatively shown in Fig. 4(a) for  $\gamma = 10$ . We observe that the critical feedback level ( $k_C$ ) tends to increase with decreasing  $\alpha$ , up to one order of magnitude. We remark that an expectation of threshold reduction with vanishing  $\alpha$  was provided in [21, 28], but the analysis was for a diode laser ( $\gamma \ll 1$ ) and grounded on its peculiar dynamics (i.e. ruled by the relaxation oscillations).

Actually, a limiting self-consistency value for  $k_C$  is also imposed by Eq. (3), where one can see that the LK model must have  $k < k_{\max} = \tau_c/2\tau_p$ , i.e.  $k_{\max} = 0.58$  in our set of simulations. The horizontal cutoff of the shaded region in Fig. 4(a) reflects this model limitation. Consistently with the above issue,  $k_C$  approaches a vertical asymptote with



decreasing  $\alpha$ , reaching  $k_{\max}$  for the critical value  $\alpha_c = 1.9$ , which thereby constitutes the minimum value of  $\alpha$  for instability to set on. We conclude that for  $\alpha < \alpha_c$  (shaded region in Fig. 4(a)), the CW emission is stable against any kind of instability predicted by the LK model, and we call this regime ultra stable. It is noteworthy that even under the LK approach limitations, a vast region of ultra stability can be reached by quantum cascade lasers. Our experimental parametric regime squarely falls in the predicted ultra stability region, thus justifying the absence of any instability in our experiments. We observe that although the maximum feedback strength  $k$  achievable within the LK model is  $k_{\max} = 0.58$ , in our experiment we measured a maximum value of  $k$  being 10 times smaller because of the diffraction losses associated with the high beam divergence of QCLs (an offhand estimation of which is reported in the Appendix).

How can the increase of the instability threshold be interpreted in terms of decreasing  $\alpha$ ? From the LK model, the reduction of  $\alpha$  corresponds to shifting the solitary laser line towards the laser (internal) cavity resonance. That causes a smaller number of external cavity modes to experience significant gain, which may lead them to compete, hence trigger the instability, and increase the value of  $k_c$ . This scenario is confirmed by the number of CW solutions  $\omega_F$  of the steady state equation (see Eq. (3)), which in turn decreases with  $\alpha$ . Figure 4(b) supports this physical interpretation as follows: we expect that, for a given  $\alpha$ , more modes may compete when the round trip time  $\tau$  is increased, since this reduces the external spectral range, while maintaining a fixed distance between the solitary laser frequency and the internal cavity resonance. The larger set of candidates to modal competition should thus lower the instability threshold, as confirmed in Fig. 4(b) by the decrease of  $\alpha_c$  with  $\tau$  up to about 1 ns ( $L = 150$  mm).  $\alpha_c$  tends to saturate around 2 for longer cavity round trip times. These results confirm that QCLs with  $\alpha < 2$  will not experience multimode instabilities even in a very long cavity, as experimentally reported. In order to provide a possible analytical justification of this saturation behavior, we are currently looking for a relation between  $\alpha_c$  and  $\tau$  starting from the Eq. (7). We also plan to include in the LK model a more realistic gain line shape to better describe the CW multimode instability and the associated complex dynamics of the active external cavity modes.

#### 4. Conclusion

In conclusion, we experimentally demonstrate that both THz and mid-IR QCLs with OF will not undergo dynamical instabilities, such as mode-hopping, intensity pulsation or coherence collapse, up to the maximum feedback strength  $k$ . Remarkably, this is almost two orders of magnitude larger than the feedback threshold that would cause instability in a diode laser.

The theoretical analysis of the LK model provides an interpretation of such a unique behavior of QCLs, attributing it to a) their ultrafast electron relaxation time in excited subbands, which rules out the destabilization via undamped relaxation oscillations, and b) negligible  $\alpha$ -factor, that reduces the number of external cavity modes possibly concurring in CW emission destabilization. This represents the first systematic study of dynamics in QCLs with optical feedback, from both a theoretical and experimental point of view.

The results described here show that the useful range of feedback levels is not limited to the narrow range usually adopted to avoid performance degradation. Moreover, the good agreement between theory and experiments brings a fundamental step forward towards deep understanding of unipolar semiconductor laser dynamics. In particular, the increase of feedback powers still yielding stable emission and self-mixing signal, can pave the way to such OF-based applications as imaging, high precision spectroscopy and sensing, where QCLs stability of CW emission is essential for operation as simultaneous sources and detectors of infrared radiation.

## Appendix

We provide an estimation of the maximum feedback level achievable in the experiment with QCLs subject to optical feedback. Although in the following we will concentrate on the THz QCL case, a similar estimation holds true in the case of mid-IR QCL.

In the framework of the LK model, the feedback strength parameter  $k$  is defined by the following relation:

$$k = \varepsilon \sqrt{\frac{R_{\text{ext}}}{R}} (1 - R) \quad (9)$$

where  $R_{\text{ext}}$  and  $R$  represents the reflectivity of the external target and the laser exit facet, respectively (experimental values:  $R_{\text{ext}} = 0.9$  and  $R = 0.3$ ); the coupling factor  $\varepsilon = \sqrt{P_F/P} < 1$  accounts for coupling losses into the external cavity, where  $P$  is the power emitted by the THz QCL, and  $P_F$  is the power re-injected into the laser after a cavity round trip. Since the laser facet is much smaller than the wavelength, the emitted radiation is characterized by high divergence, hence paraxial optics cannot be applied to the calculation of the coupling factor. Alternatively, we can get an estimation of  $\varepsilon$  by assimilating the QCL to a point-like source of spherical waves. If we further approximate the surface of the first parabolic mirror that collects and collimates the emitted radiation to that of a spherical cap of the same diameter  $D$ , the power  $P_p$  of the collimated beam is:

$$P_p = \frac{2\pi f (f - \sqrt{f^2 - (D/2)^2})}{2\pi f^2} = 0.21P \quad (10)$$

where  $f$  represents the mirror focal length. Neglecting any further loss in free space propagation, additional losses are met when the feedback beam is focused onto the laser facet. Assimilating the laser facet to a Gaussian aperture of radius  $a = 5\mu\text{m}$  (typical value), an experimentally estimated waist of  $w = 150\mu\text{m}$  yields to a re-injected power  $P_F$  given by

$$P_F = (1 - \exp(-2a^2/w^2))P_p = 0.0025P_p. \text{ Hence, we have } \varepsilon = \sqrt{\frac{P_p}{P}} \sqrt{\frac{P_F}{P_p}} = 0.02.$$

Finally, from expression (9) we derive a maximum feedback strength  $k = 0.03$  which, despite the crude approximations adopted, meets the order of magnitude of that we measured in the experiment, thus supporting the claims of intrinsic stability at any value of feedback power achievable in quantum cascade lasers.

## Acknowledgments

This work was supported by partial financial support from MIUR – PON01-2238, PON02-0576 INNOVHEAD and MASSIME. The authors L.L.C. and M.B. acknowledge funding by National Fibr Project PHOCOS (Project n. RBFR08E7VA). M.S.V. acknowledges financial support of the Italian Ministry of Education, University, and Research (MIUR) through the program FIRB 2010 - RBFR10LULP “Fundamental research on terahertz photonic devices”. The authors acknowledge A. Tredicucci for the design of THz-QCLs and useful discussions.